The Astrophysical Journal, 664: L131–L134, 2007 August 1

GLOBAL CORONAL MASS EJECTIONS

Andrei N. Zhukov[1,2] and Igor S. Veselovsky[2,3]
Received 2007 April 5; accepted 2007 June 18; published 2007 July 20

ABSTRACT

Observations of the low solar corona in the extreme ultraviolet and in soft X-rays evidence a close relationship of coronal dimmings and coronal mass ejections (CMEs). Dimmings are usually interpreted as places of plasma evacuation during a CME. We characterize a CME by the apparent angular extent of associated dimmings above the solar limb and define a global CME as a CME with the total apparent extent of limb dimmings of more than 180°. Several examples of global CMEs are discussed. All the global CMEs identified up to now are fast full-halo CMEs associated with X-class flares (if they originate on the front side of the Sun). We demonstrate that global CMEs involve an eruption of several magnetic flux systems distributed on a large spatial scale comparable to one-half of the solar disk (true angular width around 180°). We discuss possible interpretations of the global CME phenomenon and challenges it presents to CME modeling. Our results suggest a nonlocal nature of the CME eruption mechanism.

Subject headings: Sun: corona — Sun: coronal mass ejections (CMEs)

1. INTRODUCTION

The mechanism of coronal mass ejections (CMEs) is a major puzzle in the physics of the solar corona. Theoretical investigations still cannot account for all the diverse manifestations of this energy release process in the solar atmosphere. According to the current paradigm, the coronal magnetic field plays a dominant role in the CME eruption process (see, e.g., a recent review by Forbes et al. 2006). The initial magnetic field configuration is assumed to be that of a sheared arcade or a flux rope inside an arcade; i.e., it is essentially bipolar (as can be seen in photospheric magnetograms). Due to an instability or a loss of equilibrium process that remains to be identified (magnetohydrodynamic catastrophe, magnetic flux emergence or cancellation, etc.), the preeruptive magnetic field starts to rise. If the flux rope did not exist prior to the eruption, it is formed via the magnetic reconnection of the arcade's field lines. During the rise of the flux rope, the field lines of the overlying arcade reconnect in the current sheet below the flux rope, decreasing the restraining effect of the arcade and increasing the magnetic pressure force directed upward.

Correspondence of different CME signatures observed in the solar atmosphere to models is discussed by Hudson & Cliver (2001). The ejection of a flux rope leaves behind the bipolar post-eruption arcade that is well observed in soft X-rays (SXRs) and extreme ultraviolet (EUV). Another important and frequent CME signature is a coronal dimming (e.g., Rust & Hildner 1976; Sterling & Hudson 1997; Thompson et al. 2000). Dimming is observed as a temporary (around one or several hours) decrease of coronal brightness near the eruption site, typically seen in SXRs and EUV. Dimmings are usually interpreted as a consequence of removal of coronal mass during the CME eruption (Sterling & Hudson 1997; Harrison et al. 2003; Zhukov & Auchère 2004). Often a dimming appears as a transient coronal hole (TCH)—its appearance resembles that of coronal holes. Sometimes dimmings (and TCHs in particular) appear in pairs, suggesting that such a double (twin) dimming represents the footpoints of an ejected interplanetary flux rope (Webb et al. 2000).

Modern CME theories usually consider the CME initiation process as taking place locally, i.e., in a relatively small (of the order of the active region size) part of the solar corona with the bipolar field configuration. Even in the breakout model (Antiochos et al. 1999), which requires multipolar magnetic field, the opening of field lines has a local character: only the middle flux system erupts. There is, however, increasing evidence that CMEs may involve structures on a larger spatial scale (e.g., Manoharan et al. 1996; Webb et al. 1997; Delannée & Aulanier 1999; Thompson et al. 2000; Khan & Hudson 2000; Veselovsky et al. 2004; Zhou et al. 2006). Thompson et al. (2000) described the occurrences of extended dimming areas that map out well the apparent "footprint" of CMEs observed by a coronagraph. These dimmings appear not only in the erupting active region but involve adjacent transequatorial structures as well. It was suggested (e.g., Delannée & Aulanier 1999; Wang et al. 2002) that erupting low-lying bipolar field region (of an active region size) may push up the overlying transequatorial loops and make them erupt as well. Dimmings then appear both in the erupting active region and at the footpoints of erupting transequatorial loops. Zhou et al. (2006) reported a large extent of magnetic structures involved in Earth-directed CMEs. These structures, however, are again either bipolar or involve an active region and a transequatorial loop system.

In this Letter we report on the observations of CMEs with associated coronal dimmings on a global spatial scale and discuss implications of these observations on CME theories.

2. OBSERVATIONS

The process of CME initiation in the low corona can be observed by the Extreme-Ultraviolet Imaging Telescope (EIT; see Delaboudinière et al. 1995) on board the *Solar and Heliospheric Observatory* (*SOHO*). As we mentioned in § 1, one of the key CME-associated phenomena is a coronal dimming that can also be observed above the solar limb (e.g., Thompson et al. 2000).

We define a global CME as a CME that has associated dimmings above the limb extending to more than 180° in apparent position angle around the solar disk. This apparent angular extent of dimming above the limb depends on its true angular width and its location on the Sun. Our criterion allows us to identify CMEs that

[1] Royal Observatory of Belgium, B-1180 Brussels, Belgium; Andrei.Zhukov@sidc.be.
[2] Skobeltsyn Institute of Nuclear Physics, Moscow State University, 119992 Moscow, Russia; veselov@dec1.sinp.msu.ru.
[3] Space Research Institute, Russian Academy of Sciences, 117997 Moscow, Russia.

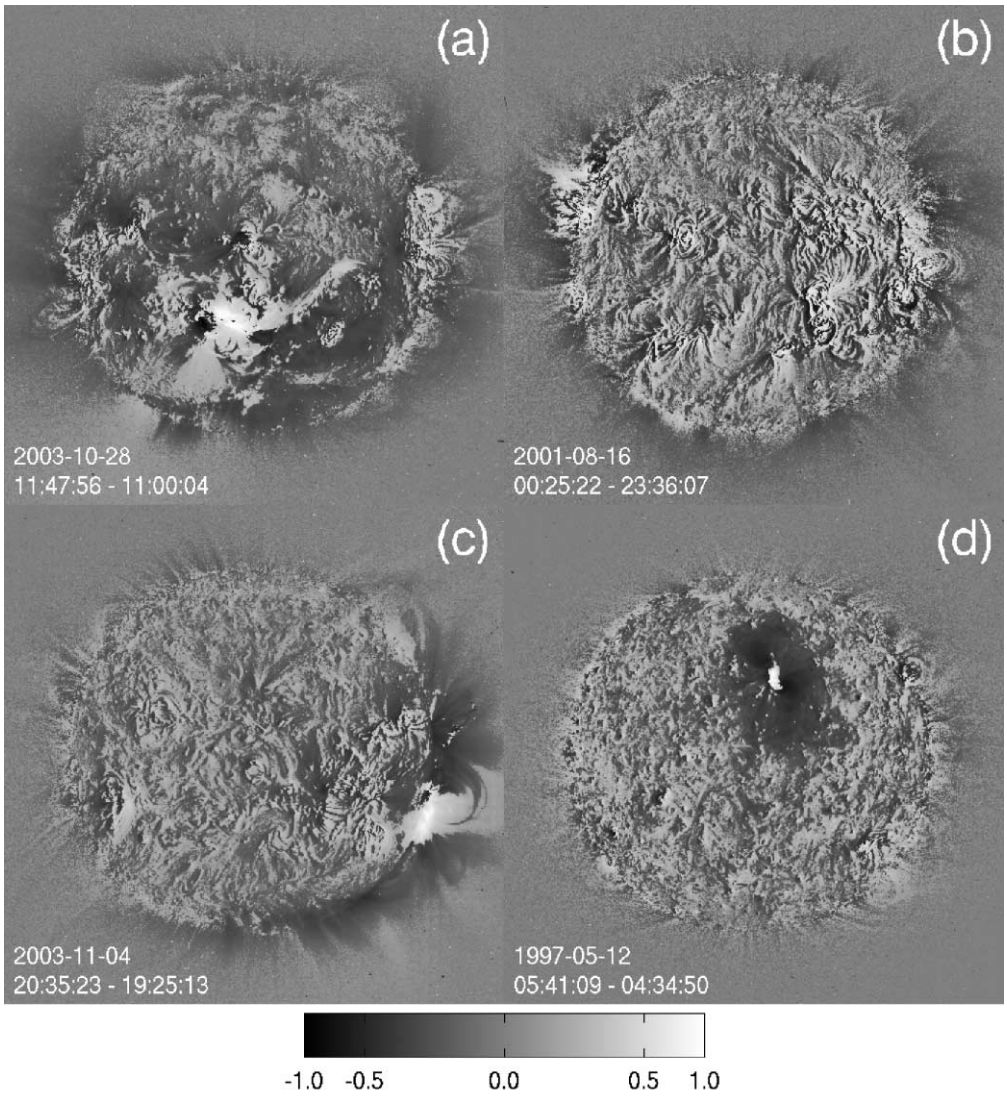

FIG. 1.—*SOHO* EIT difference images taken in the Fe XII bandpass (195 Å) showing coronal dimmings associated with global CMEs originating from (*a*) the front side, (*b*) the far side, and (*c*) the limb. For comparison, panel (*d*) shows a dimming associated with a nonglobal CME. The last preeruption image was subtracted from a post-eruption image, and the resulting base difference image was logarithmically scaled to the absolute value of the minimal brightness difference over the image. All times in this Letter are UT. North is at the top and west to the right.

are powerful enough to involve areas around at least a half of the solar disk (true angular width around 180°). In such events the location of the dimming center near the center of the solar disk (on the front or far side) favors the apparent width of around 360°, and its location on the limb leads to the apparent width of around 180°. Our threshold of 180° is somewhat arbitrary, but it is restrictive enough to allow us to select truly global events. Indeed, a typical angular size of a limb CME is around 50° (St. Cyr et al. 2000). As dimmings often map quite well to white-light CMEs (Thompson et al. 2000), we expect that the angular width of the corresponding typical dimming would not exceed this value. For CMEs originating far from the limb there is often no limb dimming at all.

Several examples of dimmings associated with global CMEs are illustrated in Figure 1 showing base difference images taken by EIT in the Fe XII bandpass (195 Å). Dimmings can be seen as dark areas with the size of an average active region or larger. Some areas on the solar disk look noisy in difference images (adjacent dark and bright features) because of solar rotation and small-scale evolution. Coronal dimming is a dynamic phenomenon, and "snapshots" like those shown in Figure 1 may exhibit only a part of dimmed regions. Figure 1*a* shows the dimmings associated with a front-side CME. Together with dimmings above the east, south, southwest and northwest limbs (the overall apparent angular extent of limb dimmings is almost 360°), extensive dimmings can be also seen all over the solar disk. Figure 1*b* shows dimmings associated with a far-side event. No noticeable dimming can be seen on the disk, but limb dimmings are visible from northeast to the south and to the northwest limb. The overall apparent angular extent of this dimming is around 270°. Figure 1*c* shows dimmings associated with a west limb CME. Dimmings are well seen from the northwest to the south and southeast limbs (apparent angular extent around 190°). For comparison, Figure 1*d* shows a dimming associated with a nonglobal CME. No noticeable limb dimming can be seen, and the dimming on the disk is localized to the vicinity of the erupting active region.

Figure 2 shows contours of a photospheric magnetogram

taken by the Michelson Doppler Imager (MDI; see Scherrer et al. 1995) on board *SOHO*, together with an EIT base difference image of a global coronal dimming. It can be seen that this eruption involves multiple magnetic flux systems. Apart from two compact darkest dimmings next to the erupting active region (NOAA AR 0486) corresponding to TCHs (i.e., probable footpoints of the ejected flux rope), a large dimming can be seen between NOAA ARs 0488 and 0487 and farther to the east. Another large dimming is located between the NOAA ARs 0486 and 0484, farther to the south around the NOAA AR 0492 and in the large-scale bipolar region in southern hemisphere. More dimmings can be seen to the east of the NOAA AR 0486 and at remote locations, like a large region just to the south of the north polar coronal hole and a dimming "lane" going from this northern dimming toward the NOAA AR 0484. We note that remote dimmings correspond to the disappearance of structures in the quiet Sun and structures connecting active regions rather than active region loops. The dimming pattern is complicated and extended over large areas of the solar surface that are comparable to one-half of the visible solar disk (true angular width around 180°) and belong to different magnetic flux systems. The true area of the dimming can be even larger than that shown in Figure 2 as the flare light scattered in the telescope overlaps some dimmings. Evolution of dimmings (cf. Figs. 2 and 1*a*) demonstrates a dynamic nature of the phenomenon.

Table 1 lists properties of global CMEs that we have identified using LASCO (Large Angle Spectroscopic Coronagraph; see Brueckner et al. 1995) and EIT data taken during the 23rd solar cycle. Global CMEs are rare events associated with strong flares (X1.3 and higher if not on the far side of the Sun). However, of 13 flares stronger than X5 that were observed by EIT in 1997–2006, only six were associated with global CMEs (in remaining events the apparent extent of limb dimmings was large but below the 180° threshold). There exists a continuous distribution of dimming sizes (from very small to very large), and global CMEs correspond to the extreme tail of this distribution, having true angular width of dimmings around 180°. As dimmings are not observed in coronal holes, the occurrence of global CMEs during the minimum and the rising phase of the solar cycle seems to be unlikely because of large polar coronal holes that constrain available angular span above the limb. It is possible that more global CMEs may be identified via a careful inspection of the EIT data, so this number—10 global CMEs (listed in Table 1)—should be considered as a lower limit on their occurrence in 1997–2006.

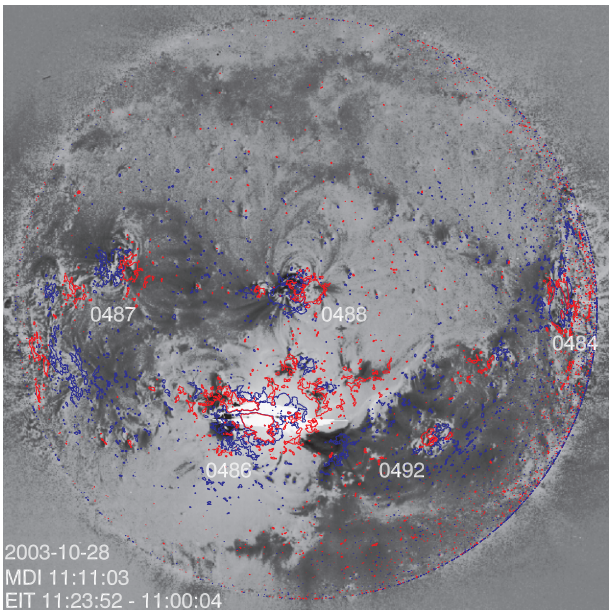

FIG. 2.—*SOHO* EIT difference image taken in the Fe XII bandpass (195 Å) showing coronal dimmings associated with a global CME on 2003 October 28 (cf. Fig. 1*a*). Red (blue) contours correspond to the photospheric magnetic field of +20 G (−20 G) in the nearly simultaneous line-of-sight magnetogram taken by *SOHO* MDI. Several active regions are marked with their NOAA numbers.

As can be seen from Table 1, global CMEs are fast (with speeds more than 1250 km s^{-1}) full-halo CMEs with very high values of the kinetic energy. It is probable that in cases of far-side global CMEs a strong flare occurred on the far side of the Sun, so during such extreme events a huge amount of the free energy is released in the form of both kinetic and radiative energy. We also note that active regions exhibiting very strong flaring activity (NOAA ARs 0486 and 0720) may produce several global CMEs during their lifetime.

TABLE 1
EXAMPLES OF GLOBAL CMES IN 2000–2005

CME Start Time[a]	CME Speed (km s^{-1})	CME E_{kin}[b] (erg)	CME AW[c] (deg)	Dimming Time[d]	Extent[e] (deg)	Flare[f]	Active Region[g]
2000 Jul 14, 10:54	1674	1.9×10^{32}	360	10:58	210	X5.7, 10:24	9077; N22°, W07°
2001 Apr 6, 19:30	1270	6.8×10^{31}	360	19:59	190	X5.6, 19:21	9415; S21°, E31°
2001 Aug 15, 23:54	1575	1.3×10^{32}	360	00:25	270	None	Back side
2002 Jul 16, 16:02	1636	...	360	16:35	280	None	Back side
2003 Oct 28, 11:30	2459	1.2×10^{33}	360	11:47	350	X17.2, 11:10	0486; S16°, E08°
2003 Oct 29, 20:54	2029	3.4×10^{32}	360	21:24	280	X10.0, 20:49	0486; S15°, W02°
2003 Nov 2, 17:30	2598	1.6×10^{32}	360	17:59	190	X8.3, 17:25	0486; S14°, W56°
2003 Nov 4, 19:54	2657	6.1×10^{32}	360	20:35	190	X28.0, 19:50	0486; S19°, W83°
2005 Jan 15, 23:06	2861	...	360	23:11	200	X2.6, 23:02	0720; N15°, W05°
2005 Jan 19, 08:29	2020	...	360	08:46	210	X1.3, 08:22	0720; N15°, W51°

NOTE.—CME start time, speed, kinetic energy and angular width are taken from the CME catalog (see Yashiro et al. 2004).
[a] First appearance of the CME in the LASCO C2 field of view.
[b] Estimated lower limit of the CME kinetic energy.
[c] Angular width (AW) of the CME as seen by LASCO.
[d] Time of maximal extent of the dimming above the limb.
[e] Maximal overall apparent angular extent of dimmings above the limb.
[f] *GOES* soft X-ray flare magnitude and peak time.
[g] NOAA number of the active region where the flare occurred and its coordinates. For two far-side events a prominent active region was detected in MDI far-side images.

3. DISCUSSION AND CONCLUSIONS

To explain the global character of CMEs reported in § 2 is a challenging problem. It seems plausible that the configuration of global dimmings reflects the configuration of the large-scale coronal magnetic field. A comparison of dimmings with the coronal field extrapolated from photospheric magnetograms using potential models was performed rather qualitatively (e.g., Delannée & Aulanier 1999; Wang et al. 2002). It is also uncertain to what extent potential models can adequately describe the coronal magnetic field before such a global eruption. Unfortunately, our understanding of the global configuration of the coronal magnetic field and its evolution during eruptions is still very poor as direct measurements of the coronal field are very difficult.

Comparison of dimmings with modeled coronal magnetic field was also performed only for simplest cases of a system comprising an active region and transequatorial loops. A straightforward interpretation proposed for such events invokes pushing the overlying (often transequatorial) magnetic flux by the main erupting flux of the active region (Delannée & Aulanier 1999; Wang et al. 2002; Liu et al. 2006), leading to the opening of large-scale overlying loops. However, in the example shown in Figure 2 the configuration of multiple dimmings is complicated, and its overall multipolar magnetic topology is uncertain. It is also not clear why global CMEs do not occur more often as there is nearly always an overlying flux system.

Khan & Hudson (2000) suggested that a large-scale coronal wave (usually observed as an EIT wave) propagating from an erupting active region may cause the destabilization of the adjacent transequatorial loop system and ultimately its opening. However, when interaction of an EIT wave with coronal structures was observed at high spatio-temporal resolution, it was shown to result rather in loop oscillations and not in their eruption (Wills-Davey & Thompson 1999). In addition, strong global EIT waves (as in the classical event of 1997 May 12) are rather usually associated with localized dimmings (see Fig. 1d) and propagate further than the dimming edge (Zhukov & Auchère 2004). An alternative model of EIT waves, interpreting them as signatures of consecutive opening of field lines during the CME lifting (Chen et al. 2002), looks promising for the investigation of global dimmings but needs to be applied to a multipolar (on a large scale) configuration of the coronal magnetic field. Another mechanism, a successive reconnection between the expanding skirt of the CME's magnetic field and quiet-Sun loops (as suggested by Attrill et al. 2007), still has to be demonstrated in a numerical model.

Although the eruption of a global CME involves multiple magnetic flux systems, we do not consider this fact as evidence of magnetic breakout (Antiochos et al. 1999). In the breakout configuration two additional bipolar flux systems serve to facilitate the eruption of a central bipolar region but do not erupt themselves. It is important to note that in most of the CME events (if not all of them), including all global CMEs listed in Table 1, there is at most one post-eruption arcade (visible as a long-duration flare in SXRs), although multiple magnetic flux systems may erupt. The interplay between global (e.g., dimmings) and local (e.g., post-eruption arcade) phenomena in the process of energy release during CMEs is not clear.

We can only speculate about subphotospheric drivers and the accumulation of free energy in the solar atmosphere that may be involved in the global CME initiation and development. They may be related to global electric currents and circuits connecting solar interior and corona. These processes remain to be investigated.

Another interpretation of dimmings (albeit an unlikely one, as shown, e.g., by Harrison et al. 2003; Zhukov & Auchère 2004) invokes changes of plasma temperature. However, even if this interpretation is correct, it is difficult to envision how a temperature change can have such a global character.

In conclusion, we presented several examples of global CMEs characterized by a very large extent of coronal dimmings. They correspond to the ejection of plasma from multiple interconnected large-scale coronal magnetic flux systems. Dimmings may thus be considered an important nonlocal manifestation of the CME initiation process and need to be described in a realistic CME model.

EIT, MDI, and LASCO data have been used courtesy of the *SOHO* EIT, *SOHO* MDI and *SOHO* LASCO consortiums, respectively. The CME catalog is generated and maintained at the CDAW Data Center by NASA and The Catholic University of America in cooperation with the Naval Research Laboratory. *SOHO* is a project of international cooperation between ESA and NASA. A. N. Z. acknowledges support from the Belgian Federal Science Policy Office through the ESA-PRODEX programme. The work of I. S. V. was supported by Russian Foundation for Basic Research grants 07-02-07012, 06-05-64500, Russian Academy of Sciences Programs P30 and OFN 16 and Interdisciplinary MSU Program. This study has been partially supported by the INTAS grant 03-51-6206.

REFERENCES

Antiochos, S. K., DeVore, C. R., & Klimchuk, J. A. 1999, ApJ, 510, 485
Attrill, G. D. R., Harra, L. K., van Driel-Gesztelyi, L., & Démoulin, P. 2007, ApJ, 656, L101
Brueckner, G. E., et al. 1995, Sol. Phys., 162, 357
Chen, P. F., Wu, S. T., Shibata, K., & Fang, C. 2002, ApJ, 572, L99
Delaboudinière, J.-P., et al. 1995, Sol. Phys., 162, 291
Delannée, C., & Aulanier, G. 1999, Sol. Phys., 190, 107
Forbes, T. G., et al. 2006, Space Sci. Rev., 123, 251
Harrison, R. A., Bryans, P., Simnett, G. M., & Lyons, M. 2003, A&A, 400, 1071
Hudson, H. S., & Cliver, E. W. 2001, J. Geophys. Res., 106, 25199
Khan, J. I., & Hudson, H. S. 2000, Geophys. Res. Lett., 27, 1083
Liu, C., Lee, J., Deng, N., Gary, D. E., & Wang, H. 2006, ApJ, 642, 1205
Manoharan, P. K., van Driel-Gesztelyi, L., Pick, M., & Demoulin, P. 1996, ApJ, 468, L73
Rust, D. M., & Hildner, E. 1976, Sol. Phys., 48, 381
Scherrer, P. H., et al. 1995, Sol. Phys., 162, 129
St. Cyr, O. C., et al. 2000, J. Geophys. Res., 105, 18169
Sterling, A. C., & Hudson, H. S. 1997, ApJ, 491, L55
Thompson, B. J., Cliver, E. W., Nitta, N., Delannée, C., & Delaboudinière, J. P. 2000, Geophys. Res. Lett., 27, 1431
Veselovsky, I. S., et al. 2004, Cosmic Res., 42, 435
Wang, T., Yan, Y., Wang, J., Kurokawa, H., & Shibata, K. 2002, ApJ, 572, 580
Webb, D. F., Kahler, S. W., McIntosh, P. S., & Klimchuk, J. A. 1997, J. Geophys. Res., 102, 24161
Webb, D. F., Lepping, R. P., Burlaga, L. F., Deforest, C. E., Larson, D. E., Martin, S. F., Plunkett, S. P., & Rust, D. M. 2000, J. Geophys. Res., 105, 27251
Wills-Davey, M. J., & Thompson, B. J. 1999, Sol. Phys., 190, 467
Yashiro, S., Gopalswamy, N., Michalek, G., St. Cyr, O. C., Plunkett, S. P., Rich, N. B., & Howard, R. A. 2004, J. Geophys. Res., 109, 7105
Zhou, G. P., Wang, J. X., & Zhang, J. 2006, A&A, 445, 1133
Zhukov, A. N., & Auchère, F. 2004, A&A, 427, 705